Abstract for the 29th Intl Workshop on Water Waves and Floating Bodies, Osaka (Japan), March 30 April 02, 2014.

Highly nonlinear wave in tank with small density ratio.

Y.-M. Scolan[1⋆], **M. R. Karimi**[2,3,4], **F. Dias**[6,4], **J.-M. Ghidaglia**[4], **J. Costes**[4,5]
[1] Ensta Bretagne, Brest, France, [2] Gaztransport & Technigaz, Saint-Rémy-lès-Chevreuse, France, [3] Delft University of Technology, Delft, The Netherlands, [4] Ecole normale supérieure de Cachan, Cachan, France, [5] Eurobios SCB, Gentilly, France, [6] University College Dublin, Ireland

1) Introduction

Usually sloshing is simulated without accounting for the temporal and spatial variations of the ullage pressure. Yet interactions between the liquid and the gas may be noticeable. In Abrahamsen and Faltinsen (2012) the liquid and the gas are both considered as inviscid and incompressible until an air pocket is captured. Then a polytropic gas law allows to further simulate the oscillation of the entrapped pocket.

We consider here a closed two-dimensional tank in which the fully nonlinear free surface boundary conditions are solved in the framework of potential theory. The kernel of the model is described in Scolan *et al* (2007). The two fluid system is handled in the same way as in Grue *et al* (1997). The model is validated by computing the advection of a solitary wave. Theoretical, numerical and experimental data are compared.

In the present model, the interface is allowed to reach a high steepness leading eventually to overturning crests. When sharp crests are formed the model cannot be used since potential flow theory predicts a high velocity at the tip of the crest in the gas. However it is shown that gas dynamic may inhibit the development of the crest. The present results show that even with small density ratios the coupled dynamics of the two fluids is substantially modified with respect to the single fluid dynamics with vacuum above a free surface. Experimental data seem to confirm the findings.

2) Method of solution

We consider a rectangular tank with two layers of fluids which are not miscible, with Ω_g and Ω_f the corresponding fluid domains.

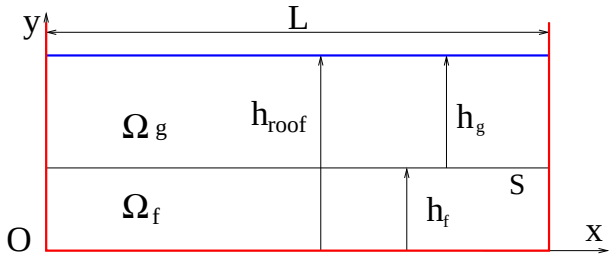

The upper part of the rectangular tank is closed with a roof which is flat at present, but could be more complex (chamfered, etc). The coordinate system is centered at the left bottom corner of the tank. The fluid in the upper layer has density ρ_g, its thickness at rest is $h_g = h_{roof} - h_f$. The fluid in the lower layer has density ρ_f and its thickness at rest is h_f. The density ratio is denoted by $r = \frac{\rho_g}{\rho_f}$. The thickness ratio is denoted by $H = \frac{h_g}{h_f}$. The flow is described with potential theory and the continuity of pressure and normal velocity is prescribed at the separation line between the two fluids without surface tension or artificial dissipation. The first application consists in validating the model with well known solutions for solitary waves that propagate along the interface. In that case both the interface deformation and the velocity potentials are given initially on the interface S. The second application consists in simulating the flow that follows from an initial deformation of the interface starting from rest.

The Method of Fundamental Solutions (MFS) is used to solve the Boundary Value Problem (BVP). That means that the velocity potential valid in a given fluid domain, is expressed as a finite summation of Green functions located at a small distance from the actual fluid boundaries but outside the considered fluid domain. Regardless the domain where it is computed, the potential is expressed as $\phi(x,y) = \sum_{i=1}^{N} q_i G(x,y,X_i,Y_i)$, where (X_i,Y_i) are the cartesian coordinates of the singularities (sources) and q_i are their intensities. By writing this equation at N markers at the interface (x_j,y_j), we obtain a linear system which is noted $\phi_j = \sum_{i=1}^{N} q_i G_{ij}$ or more simply denoted in the matrix form $\phi = Gq$. Two BVPs are posed in each fluid domain. In the lower fluid domain, on the solid boundaries, an impermeability condition is imposed. The Green function is calculated so that the impermeability conditions are implicitly accounted for. To this end the conformal mapping $w = -\cos\frac{\pi z}{L}$

is used. This transformation "flattens" the two vertical walls of the rectangular tank. The images of all solid boundaries are hence located along the horizontal axis. Then by adding to the Green function its image with respect to this horizontal axis, the resulting Green function verifies the Neumann conditions along that plane. In the upper fluid domain, we proceed the same way but the conformal mapping is $w = \cos\frac{\pi}{L}(z - ih_{roof})$. This transformation turns the semi infinite strip directed downwards (in the physical plane) into the upper half space of the transformed w plane. The combination of two conformal mappings, as done in Scolan (2010), allows to consider almost any kind of geometries provided that they match along the vertical walls.

At the interface, we have to verify the continuity of pressure $p_f = p_g$ and normal velocity $\vec{\nabla}\phi_f \cdot \vec{n} = \vec{\nabla}\phi_g \cdot \vec{n}$. The interface is defined by a set of Lagrangian markers which move with their local velocity. As done in Grue *et al* (2007), a set of pseudo-markers are tracked along the interface. Their cartesian coordinates are denoted by $\vec{x}$. They are convected with the weighted velocity $\vec{V} = (1-\alpha)\vec{\nabla}\phi_f + \alpha\vec{\nabla}\phi_g$ where $\alpha \in [0:1]$. By noting φ the combination of potentials $\varphi = \phi_f - r\phi_g$, the time differential equation for φ reads

$$\frac{\mathrm{d}\varphi}{\mathrm{d}t} = \vec{V}\cdot\left(\vec{\nabla}\phi_f - r\vec{\nabla}\phi_g\right) - \frac{1}{2}\left(\vec{\nabla}^2\phi_f - r\vec{\nabla}^2\phi_g\right) - (1-r)gy \tag{1}$$

and the markers are moved by solving the differential equation $\frac{\mathrm{d}\vec{x}}{\mathrm{d}t} = \vec{V}$. The numerical algorithm is organized as a loop in time where we first update φ and $\vec{x}$ by solving their associated time differential equation. Then we compute the source intensities by solving the linear system

$$\begin{pmatrix} G_f & -rG_g \\ G_{f,n} & -G_{g,n} \end{pmatrix}\begin{pmatrix} q_f \\ q_g \end{pmatrix} = \begin{pmatrix} \varphi \\ 0 \end{pmatrix} \tag{2}$$

and finally we compute the spatial derivatives of ϕ_f and ϕ_g yielding the RHS of the time differential system.

3) Solitary wave in a a two-fluid system

The literature about internal gravity waves travelling at the interface between two non-miscible fluids is abundant. The solution for nonlinear internal waves in shallow water is given in Long (1956) and many authors further studied solutions of the Euler equation. Among then Choi and Camassa (1999) showed that the travelling wave solution can be obtained from the integration of the equation

$$(\zeta_{,X})^2 = \kappa^2\frac{\zeta^2(\zeta - a^{(-)})(\zeta - a^{(+)})}{\zeta - a^{(\star)}}, \quad X = x + ct, \quad a^{(\star)} = h_g\frac{1+rH}{1-rH^2}, \quad \kappa^2 = \frac{3g}{c^2h_f^2}\frac{1-r}{rH^2-1} \tag{3}$$

and $a^{(\pm)}$ are the two roots of the equation $\zeta^2 + q_1\zeta + q_2 =$ with $q_1 = -\frac{c^2}{g} - h_g + h_f$ and $q_2 = h_f h_g\left(\frac{c^2}{c_o^2} - 1\right)$. The phase velocities are

$$c_o = \sqrt{gh_g\frac{1-r}{H+r}}, \quad c = c_o\sqrt{\frac{(h_g-a)(h_f+a)}{h_fh_g - ac_o^2/g}} \tag{4}$$

The initialization of the velocity potential follows from the mass conservation law combined to the kinematic boundary condition at the interface, yielding $\phi_{f,x}$ then ϕ_f after integrating once more in x. In order to initialize ϕ_g, the continuity of the normal velocities at the interface is used. It should be noted that the standard KdV solution is not used here since Choi and Camassa showed that the finite amplitude solitary wave is wider than the weakly nonlinear solution. The experimental results obtained by Koop and Butler (1981) confirm this trend. The so-called effective wavelength is computed. It is defined as follows

$$\lambda_I = \frac{1}{2a}\int_{-\infty}^{+\infty}\zeta(X)dX \tag{5}$$

By using the expression (3), this wavelength is calculated analytically in terms of integral elliptic functions. The figures below illustrate the results

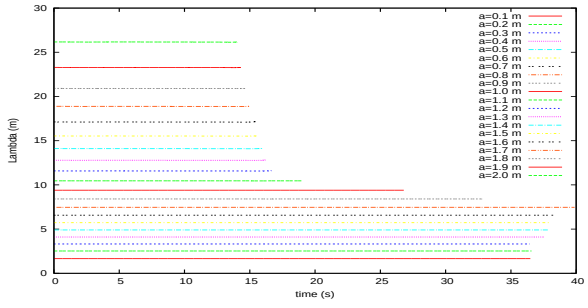

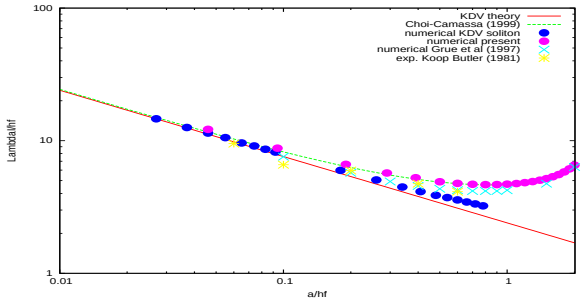

The tank is $100m$ long, the density ratio $r = 0.633$ and the depth ratio $H = 5.096$. For simplicity $h_f = 1m$ and the initial solitary wave height varies in the range $a \in [0.1m : 2m]$. The left figure shows the time variation of λ_I/h_f. It is observed that the model fails at computing the reflection of the solitary wave on the left wall for large amplitudes a. For moderate amplitudes the reflection occurs and in spite of that, the effective length is remarkably constant. The left figure above just shows that the present model simulates accurately the propagation of the solitary wave defined by the equations (3) to (4).

4) Breaking wave at a wall

The next application is much less documented even if some aspects of the problem are addressed in Laget and Dias (1997) or Dias and Vanden-Broeck (2003). We start from an initial interface deformation defined by a half gaussian centered at the right wall as illustrated below in the left figure. The roof is flat and located at $y = 1.2m$.

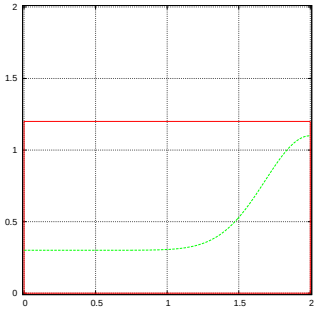

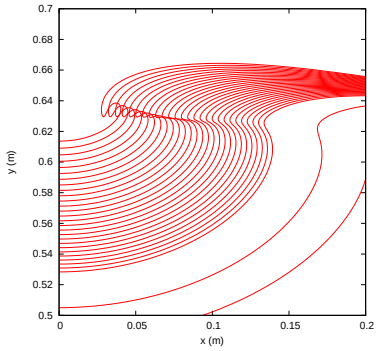

The right figure shows the last wave profiles as the crest overturns at the left wall when the density ratio r is zero. The density ratio is changed and the next figures show the last wave profiles for $r = 0.001$ and $r = 0.004$.

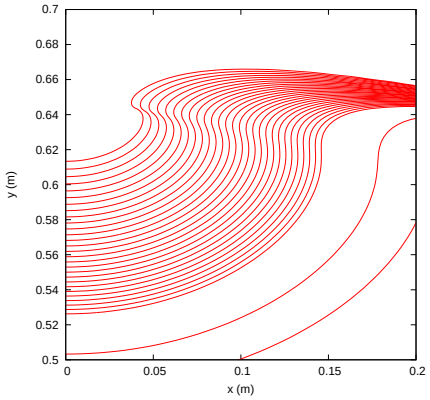

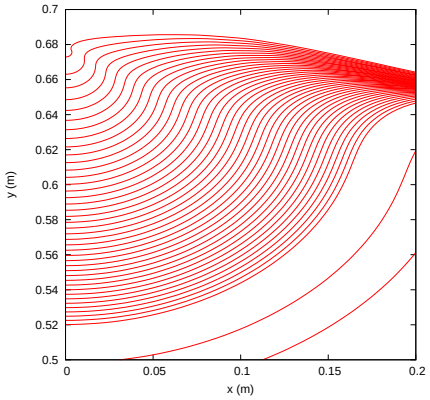

Those results show the same trend as the experimental observations made by Karimi and Brosset (2013). The next figures show the wave profiles for different density ratios $r = 0.0003$, 0.0012, 0.002 and 0.004 from left to right. It should be noted that strict comparisons are not yet possible. The reasons are 1) the geometry of the tank in the experimental setup is different from the computed solution, and 2) the experimental wave is generated by the tank motion, while the computed solution originates from an initial deformation of the interface.

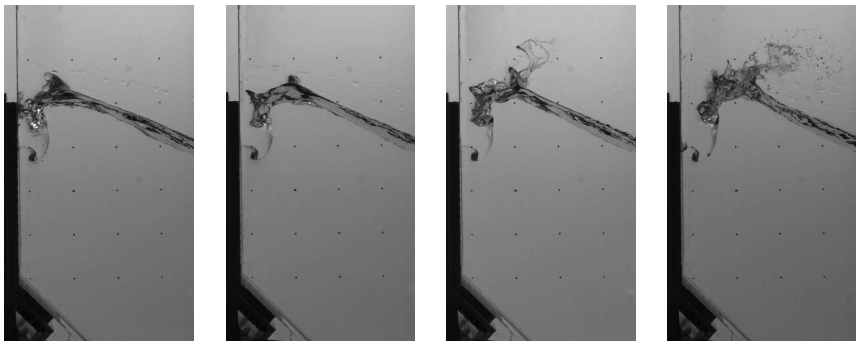

Courtesy of Gaz-Transport et Technigaz

The velocity fields in liquid and gas are shown in the next (left) figure for $r = 0.001$ at time $t = 0.67s$. In the right figure, the velocities in liquid and gas are plotted at the 280 markers which define the interface. It is shown that the amplitude of the velocity in the gas reaches greater values than in the liquid, especially where the curvature radius of the interface decreases. That can explain why fragmentation of the fluid occurs precisely there as it is observed experimentally by Lugni *et al* (2010).

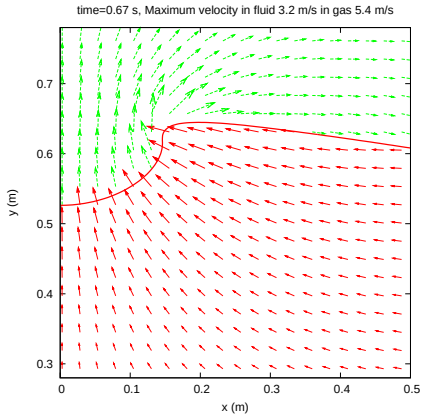

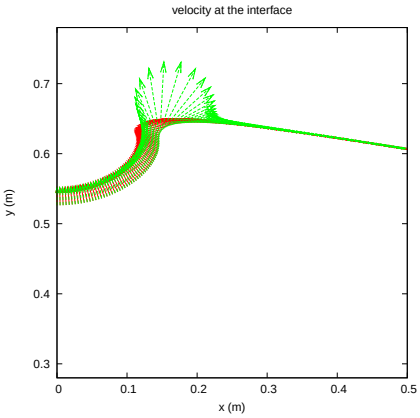

5) Conclusion

It is questionable to assert that a potential flow model can predict accurately the dynamic of the interface between two fluids with small density ratio. As an intermediate step we can reasonably consider that the velocity field presently computed in the gas could be used as initial conditions for more sophisticated codes where the compressibility of the gas is better handled.

6) References

• Abrahamsen B.C. & Faltinsen O.M., 2012, A numerical model of an air pocket impact during sloshing Applied Ocean Research, Volume 37, pp 54-71.

• Choi W. and Camassa R., 1999, Fully nonlinear internal waves in a two-fluid system. Journal of Fluid Mechanics, 396, pp 1-36.

• Dias F. & Vanden-Broeck J.-M., 2003, On internal fronts, J. Fluid Mech. 479, pp. 145–154.

• Grue J., Friis H.A., Palm E. and Rusas P.O. 1997, A method for computing unsteady fully nonlinear interfacial waves. Journal of Fluid Mechanics, 351, pp 223-252.

• Laget O. & Dias F. 1997, Numerical computation of capillarygravity interfacial solitary waves J. Fluid Mech. vol. 349, pp. 221–251.

• Long, R. R. 1956, Solitary waves in one and two fluid systems. Tellus 8, 460.

• Lugni C., M. Miozzi, M. Brocchini, O. M. Faltinsen, 2010, Evolution of the air cavity during a depressurized wave impact. I. The kinematic flow field Physics of Fluids, vol. 22.

• Karimi R. & Brosset L. 2014, Global and Local Effects of Gas-Liquid Density Ratio on Shape and Kinematics of Sloshing Waves and Scaling Considerations, IWWWFB29, Osaka, Japan.

• Koop, C. G. & Butler, G., 1981, An investigation on internal solitary waves in a two-fluid system. J. Fluid Mech. 112, 225–251.

• Scolan Y.-M., 2010, Some aspects of the flip-through phenomenon: A numerical study based on the desingularized technique, Journal of Fluids and Structures 26 (6), 918-953.

• Scolan, Y.M., Kimmoun, O., Branger, H. & Remy, F., 2007, Nonlinear free surface motions close to a vertical wall. Influence of a local varying bathymetry. IWWWFB22, Plitvice, Croatia.